Physics Letters A 373 (2009) 1155–1158

Contents lists available at ScienceDirect

Physics Letters A

www.elsevier.com/locate/pla

Transverse waves and vortex fields in non-relativistic fluid flows

D.F. Scofield [a], Pablo Huq [b,*]

[a] Department of Physics, Oklahoma State University, Stillwater, OK 74076, USA
[b] College of Marine and Earth Studies, University of Delaware, Newark, DE 19716, USA

ARTICLE INFO

Article history:
Received 2 December 2008
Accepted 22 January 2009
Available online 29 January 2009
Communicated by F. Porcelli

PACS:
47.75.+f

Keywords:
Geometrodynamics
Acoustic spacetime
Relativistic fluid dynamics
Magnetohydrodynamics

ABSTRACT

A special acoustic spacetime generalization of the Navier–Stokes equations including a fluid vortex field is presented. This spacetime theory is verified by experimental measurements at low speeds of the order of meters/sec. The vortex field explains the enhanced energy dissipation and the persistence of transverse wave mode excitations.

1. Introduction

Acoustic spacetimes have been used to develop hydrodynamical models of general relativistic effects by Unruh [1,2] and others, see Ref. [3] for a recent review. By restricting these spacetimes to special acoustic spacetimes (SASTs), we have developed a SAST theory of viscous fluid dynamics called gemetro-fluid dynamics (GFD). A SAST naturally incorporates a limit to the maximum speed of transverse waves. These are composed of the wave modes of the vortex field. We show how the GFD generalizes the Navier–Stokes theory (NST) to include the vortex field, thereby promoting this generalization of the NST to a classical SAST field theory. Balancing inertial, viscous and vortex stress–energies then leads to the fluid spacetime theory that we verify using experimental measurements at low speeds of the order of meters per second.

The vortex field introduced here is an exact fluid analogue of an electromagnetic field. The present Letter shows that travelling wave modes of the vortex field fluid flows are similar to electromagnetic wave modes of an electromagnetic field.

A quantifiable manifestation of transverse wave modes of the vortex field in experimental work is elevated energy loss [4]. In contrast, energy loss required for longitudinal waves is small as little work is needed for their propagation. Small amplitude, short wavelength transverse waves are evanescent involving little energy expenditure. Large amplitude, transverse waves, however, require larger energy expenditure to propagate, can be long lived and, thereby, significantly affect the fluid dynamics. Because of the coupling of the vortex field to the mean flow, these waves often move at or near the average stream velocity of the main flow.

Evidence of transverse waves is found in the experiments of White [5], Taylor [6] and subsequent researchers [7] on flow in helical pipes of circular cross-section. In these flows, the transverse waves generated are so pronounced that turbulent pipe flow inlet to a helical section appears to “relaminarize” [8–10]. Furthermore, on outlet to a straight section, the transverse wave excitation persists for at least a thousand pipe diameters [7]. It is natural to analyze these waves in the context of the Navier–Stokes theory (NST) but, as we show here, the NST does not explain the enhanced energy dissipation and long lifetime of transverse waves in helical pipe flow [7].

2. Vortex fields in special acoustic spacetimes

The experimental results noted above can be described as due to the excitations of a fluid vortex field in a special acoustic spacetime [4]. Because the vortex field needs a spacetime for its definition, the present theory owes much in its formulation to an understanding of the structure of relativistic fluid mechanics [11]. The vortex field can be understood from the viewpoint of NST variables. In the NST, given the Eulerian velocity field u, the vortex field $\mathring{F} = \{\omega, \zeta\}$ includes the vorticity, $\omega \to \nabla \times u$, *and* the swirl, $\zeta \to u \times \omega$, field vectors. The variables $\mathring{G} = \{\varpi, \xi\}$ are excitations of the vortex field and are linearly related to $\mathring{F}$ using fluid constitutive parameters. The components of $\mathring{F}$ and $\mathring{G}$ can be written as

* Corresponding author.
E-mail address: huq@udel.edu (P. Huq).

0375-9601/$ – see front matter
doi:10.1016/j.physleta.2009.01.048

anti-symmetric tensors. Significantly, these tensors unify the vorticity and the swirl field. One can introduce transverse waves into the NST and calculate the response of fluid viscosity and momentum on those waves [12]. To fully include the interaction of the fluid and the wave field requires the development of a theory including the transverse wave modes of the vortex field as part of the stress–energy balance.

Three types of transverse wave (TW) modes are possible as described by the triad $\{\omega, \zeta, u\}$. These waves arise in the general decomposition of wave systems with local cylindrical symmetry [13, Sec. 9.18] which holds for helical flow when ratio d/D of the pipe diameter d to the projected helix diameter D is small. The three waves are named by the components of the wave lying in the transverse-to-the-flow direction in analogy to electromagnetic field theory [13]. They are transverse vorticity–swirl (TVS), transverse vorticity (TV), and transverse swirl (TS) waves. The TVS waves do not propagate in a bounded medium. TV and TS waves take the form of cylinder functions, i.e., proportional to $J_n(p_{nm}r/a)\cos(n\phi)\exp(-i\alpha_{nm}z)$ where r is the transverse radial coordinate, ϕ the transverse angular coordinate, and z the streamwise coordinate for a pipe of diameter $d = 2a$. Here $J_n(x)$ is the nth Bessel function. The TV modes are computed to meet the zero-slip condition $J_n(p_{nm}) = 0$. These modes form a basis set for expanding any radial velocity profile in these flows $u(r) = \sum_{m=1}^{\infty} A_m J_n(p_{nm}r/a)$, and consequently a basis for the vortex field modes. Examples of the TV modes are illustrated alphabetically in the figure inset for $(n, m) = (1, 1), (1, 2), (2, 1), (2, 2)$. The $(1, 1)$ mode is observed in helical pipes and in the straight section down-stream of a helical pipe for more than a thousand diameters.

The theoretical existence of a vortex field in a SAST follows mathematically from the converse of the Poincaré lemma [14, p. 27] in the same way as it does in electromagnetic field theory [15]. Based on a theorem of Kiehn [16, vol. 5, p. 122], one can show for SASTs that are deformable, i.e., ones which can be slightly curved, that there are conserved 4-currents. In general, the existence of conserved currents in a SAST implies the existence of a vortex field in time varying flows. Using these properties and known results concerning the structure of the Navier–Stokes equations (NSEs) for a spacetime [11], but restricted to a SAST, one can assemble the tensor component form of the field equations for a Newtonian fluid flow with a vortex field:

$$(\tau_e - \tau_n)^{\mu\nu}{}_{;\nu} = -\mathring{F}^{\mu\nu} j_\nu, \tag{1a}$$

$$^\star\mathring{G}_{\kappa\nu} = \mathring{F}_{\kappa\nu}, \tag{1b}$$

$$\mathring{F}_{\mu\nu} = \frac{1}{2}\left(\frac{\partial A_\nu}{\partial x^\mu} - \frac{\partial A_\mu}{\partial x^\nu}\right), \tag{1c}$$

$$-\Box A_\mu = -\left(\partial_t^2 - \nabla^2\right)A_\mu = \frac{4\pi}{\bar\eta} j_\mu. \tag{1d}$$

In Eq. (1a), stating the stress-energy balance in a fluid with a vortex field, the first covariantly differentiated term is the Euler stress–energy $\tau_e^{\kappa\nu} = \rho u^\mu u^\nu + p(g^{\mu\nu} + u^\mu u^\nu)$ due to the fluid inertia. Here the SAST metric for one time and three spatial coordinates is $(g_{\mu\nu}) = \mathrm{diag}(-1, 1, 1, 1)$, $c_m = 1$. The SAST Euler equation is $\tau_{e;\nu}^{\mu\nu} = 0$. The second term on the left in Eq. (1a) $\tau_n^{\mu\nu} = \eta(\mathcal{P}_\nu^\epsilon u_{\mu;\epsilon} + \mathcal{P}_\mu^\epsilon u_{\nu;\epsilon})$ with $\mathcal{P}_{\mu\nu} = (g_{\mu\nu} + u_\mu u_\nu)$ is the Newtonian fluid stress–energy tensor of an incompressible fluid. Here the u^μ are the 4-velocity components, p is the pressure and ρ is the fluid density. The equation $(\tau_e^{\kappa\nu} - \tau_n^{\kappa\nu})_{;\nu} = 0$ is the SAST equivalent of the NSEs [11]. The contribution of the vortex field stress–energy tensor $\tau_m^{\kappa\nu} = -\mathring{F}^{i\nu} j_\nu$ is contained in the right-hand side of Eq. (1a) [17, Section 12.10]. The Lorentz force $-\mathring{F}^{i\nu} j_\nu$ forms a source of self-excitation to the flow. Eq. (1b) states the linear relation between the vortex field excitations $\hat{G}$ and the vortex field $\hat{F}$. Eq. (1c) shows the vortex field is obtained from a vector potential A satisfying wave equation (1d). The material parameter $\bar\eta^{-1}$ appearing in that wave equation gives the strength at which the vortex field is coupled to the fluid current j.

Using standard techniques [13,17] we can form a tensor $\mathring{\tau}_m^{\mu\nu}$, the fluid dynamical analogue to the Maxwell stress–energy tensor, whose components are given as.

$$4\pi\,\mathring{\tau}_m^{\mu\nu} = g^{\mu\alpha}\dot{F}_{\alpha\beta}\ \dot{F}^{\beta\nu} - \frac{1}{4}g^{\mu\nu}\dot{F}_{\alpha\beta}\ \dot{F}^{\alpha\beta}, \tag{2a}$$

$$4\pi\,\mathring{\tau}_m^{00} = \frac{1}{2}\left(\kappa^2\omega^2 + \lambda^2\zeta^2\right), \tag{2b}$$

$$4\pi\,\mathring{\tau}_m^{0j} = 4\pi\,\mathring{\tau}_m^{j0} = -(\kappa\omega \times \lambda\zeta)^j, \tag{2c}$$

$$4\pi\,\mathring{\tau}_m^{jk} = -\left(\kappa^2\omega^j\omega^k + \lambda^2\zeta^j\zeta^k\right) + \frac{1}{2}\left(\kappa^2\omega^2 + \lambda^2\zeta^2\right)\delta^{jk}. \tag{2d}$$

The vortex field $\{\omega, \zeta\}$ used in these equations is obtained from the 4-vector potential A according to Eq. (1d). Since the units of ω are inverse seconds, T^{-1}, $[\zeta] = LT^{-2}$, then for dimensional consistency we have $[\lambda] = TL^{-1}$, i.e., inverse velocity. We note that the absolute viscosity $[\eta] = [m/LT] = ET/L^3$ so that $\eta\mathring{\tau}_m^{00} = \frac{-\eta}{8\pi}(\kappa^2\omega^2 + \lambda^2\zeta^2)$ represents the energy dissipation of the vortex field. Here E represents the units of energy. The other tensor components represent momentum dissipation $\eta\mathring{\tau}_m^{0j}$ and stress dissipation $\eta\mathring{\tau}_m^{jk}$. In Eqs. (1a)–(1d) and (2a)–(2d) there have been introduced constitutive parameters $\{\kappa, \bar\kappa, \lambda, \bar\lambda, \bar\eta\}$. Only the ratios of the first and second pairs of parameters need be specified.

For comparison to experimental results, we present two relations for the energy dissipation in pipe flow using an energy-integral method [4]. From Eq. (2b), the energy dissipation due to the vortex field and the NST vorticity (without wave–wave interactions discussed below) can be written as [4]

$$\frac{d\mathcal{E}}{dt} = -\frac{32\eta F_d\langle\|u\|\rangle^2}{d^2} = -\eta\int_\Delta \left(\kappa^2\omega^2 + \lambda^2\zeta^2\right)dV \tag{3a}$$

$$\equiv -\eta\langle\|u\|\rangle^2 h_0[u]\left\{1 + \lambda^2 h_2[u]\right\}. \tag{3b}$$

In Eq. (3a), the term $-32\eta F_d\langle\|u\|\rangle^2/d^2$ gives the energy dissipation for a turbulent flow in terms of a friction factor F_d for a pipe diameter d. This is equated to the vortex field energy dissipation obtained from $\eta\mathring{\tau}_m^{00}$ using Eq. (2b). For simplicity, we now set $\kappa = 1$. In Eq. (3a) $\langle\|u\|\rangle \equiv \int_\Delta \|u\|dV$ and $h_0[u] \equiv \int_\Delta \|\omega\|^2\langle\|u\|\rangle^{-2}dV$. The Navier–Stokes dissipation contains only the ω^2 integrand in Eq. (3a) [4]. Using the relations $\omega \to \nabla \times u$ and $\zeta \to u \times \omega$, from NST, it is seen that $h_0[u]$ is a degree zero functional of the velocity (does not depend on the scale of the velocity field) and $h_2[u] \equiv \lambda^2\int_\Delta \|\zeta\|^2\|\omega\|^{-2}dV$ is a homogeneous degree two (quadratic) functional of the velocity field scale, such that $h_{n=2}[\alpha x] = \alpha^2 h_2[x]$. These relations allow one to obtain the friction factor $F_d = C_d/C_{d_0} = (d^2/32)h_0[u]\{1 + \lambda^2 h_2[u]\}$. For large enough velocity, the additional dissipation due to the vortex field scales as $\lambda^2 h_2[u]$ compared to the scaling of dissipation in a straight pipe, nominally given by $h_0[u]$.

Including the wave–wave interaction of TV and TS waves, from Eq. (2c) expressed as an energy dissipation integral, leads to the second relation

$$\frac{d\mathcal{E}}{dt} = -\frac{32\eta F_d\langle\|u\|\rangle^2}{d^2} = -\eta\lambda\int_\Delta (\zeta \times \omega)\cdot\hat{e}_z\,dV$$

$$\equiv -\eta\lambda\langle\|u\|\rangle^2 h_1[u]. \tag{4}$$

Here $h_1[u]$ is a homogeneous degree-one (linear) functional of u. This expression applies for both TS and TV waves. When both TS and TV waves interact this expression has a non-trivial value.

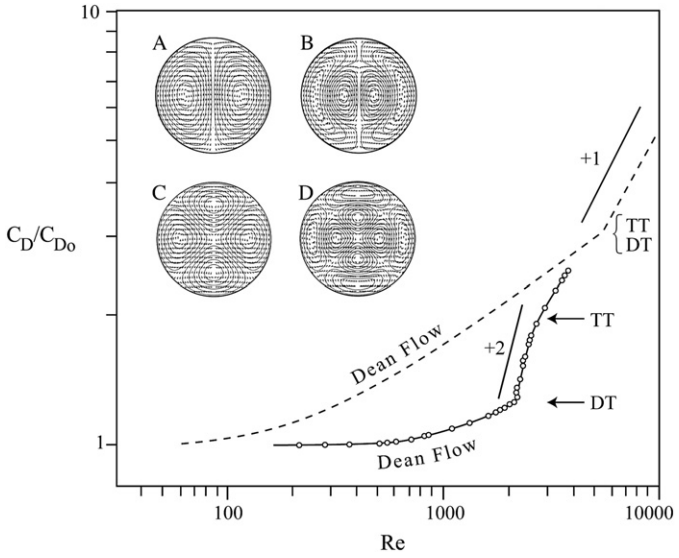

Fig. 1. Comparison of theory and experiment. Main curves for energy dissipation showing predicted (+1) and (+2) slopes due to vortex field mediated dissipation. Inset shows lower energy vortex field TV excitation modes for tubular flow.

The predictions of this theory are then linear and quadratic power laws for energy dissipation. For Eqs. (3a), (3b), the predicted dissipation dependence on the velocity field scale gives a +2 slope in a log–log plot of energy dissipation versus Reynolds number. For the wave–wave interaction, Eq. (4), the predicted dissipation dependence gives a +1 slope. An intermediate value of the slope is found when both effects are present.

Let us next compare these predictions to experimental measurements. The experimental results are reported in terms of the pressure drop factor in the pipe relative to the same length of straight pipe $F_d = C_d/C_{d_0}$ for identical flow rates. Fig. 1 plots the log (C_d/C_{d_0}) vs. log $(Re = \langle u\rangle d/(\eta/\rho))$ energy dissipation curves for two sets of pipe flow data from White [5] and Taylor [6]. Here u is the flow speed, ρ is the density, d is the pipe diameter, and η is the absolute viscosity. For helical pipe flow, there is a significant, heretofore unexplained, increase in the energy dissipation when the flow begins to vary in time. This behavior begins at the Dean-to-transitional points (DT). The solid curve is for a pipe with a curvature ratio of $d/D = 1/2050$ and for the dashed curve this ratio is 1/50. Here D is the projected diameter of the helical coil. In the data associated with the solid curve, for Reynolds numbers Re up to about 2250, the flow is in the so-called "Dean vortex" flow regime shown in Fig. 1. The transitional regime (DT-TT), occurs for $2250 < Re < 3200$ has a slope of +2. Beyond the transition-to-turbulence point (TT) the slope becomes +1. For the dashed curve data, the curve transitions directly from the Dean regime to turbulent flow with a +1 slope (beyond $Re = 5200$) passing quickly through the +2 slope transitional flow region. More extensive data sets are reported in Ref. [18]. Fitting the data in the figure gives a value of $\lambda = 0.01$ $(\mathrm{cm/s})^{-1}$ for water. The evaluation of the other constitutive parameters $\{\kappa, \bar{\kappa}, \bar{\lambda}, \bar{\eta}\}$ awaits solution to the fluid field equation and corresponding experiments.

Recent work in straight pipe flows [19–23] also shows the importance of nonlinear travelling waves in fluid dynamics as in Ref. [24]; see also [22,23,25] for recent reviews, so we expect similar transverse wave engendered energy dissipation in straight pipe experiments.

Let us now show how the present theory relates to the NST. By taking the small $\|u\|/c_m$ limit, we find [11, Chapter 15, replace c with c_m]

$$\rho\frac{\partial u^i}{\partial t} + \rho u\cdot\nabla u^i + \nabla^i p - \eta\nabla^2 u^i = -\dot{F}^{i\nu} j_\nu. \tag{5}$$

It is seen that the convective nonlinearity $u\cdot\nabla u^i$ is present. The Lorentz term $-\dot{F}^{i\nu} j_\nu$, signalling the presence of a vortex field, is also nonlinear; it contains the effects of the vorticity and swirl multiplied by the fluid velocity in the guise of fluid current j. Using the value for $\mathring{F}$ and the components of the fluid current j, one can evaluate the right-hand side of Eq. (5)

$$\left(\mathring{F}^{\mu\nu} j_\nu\right) = \begin{pmatrix} 0 & \lambda\zeta_1 & \lambda\zeta_2 & \lambda\zeta_3 \\ -\lambda\zeta_1 & 0 & \kappa\omega_3 & -\kappa\omega_2 \\ -\lambda\zeta_2 & -\kappa\omega_3 & 0 & \kappa\omega_1 \\ -\lambda\zeta_3 & \kappa\omega_2 & -\kappa\omega_1 & 0 \end{pmatrix}\begin{pmatrix} j_0 \\ j_1 \\ j_2 \\ j_3 \end{pmatrix}. \tag{6}$$

Then, from Eqs. (5) and (6) there is obtained

$$\frac{Du^i}{Dt} = \frac{\partial u^i}{\partial t} + u\cdot\nabla u^i = -\frac{1}{\rho}\nabla^i p + \frac{\eta}{\rho}\nabla^2 u^i + (\lambda c_m - 1)\zeta^i. \tag{7}$$

This reduces to the NSEs when $\lambda c_m - 1 = 0$. The term $(\lambda c_m - 1)\zeta^i$ describes the momentum due to the presence of the vortex field. It is of the same type as the $u\cdot\nabla u^i$ term. Using the NST relation $\omega \to \nabla\times u$ we also find a diffusion equation for the vorticity

$$\frac{\partial\omega^i}{\partial t} + \mathcal{L}_{\lambda c_m u}\omega^i = \frac{\eta}{\rho}\nabla^2\omega^i. \tag{8}$$

The operator $\mathcal{L}_u$ is the *Lie bracket* $\mathcal{L}_u\omega = [u,\omega] = u\cdot\nabla\omega - \omega\cdot\nabla u$. Eq. (8) describes the diffusion and convection of vorticity in the frame of reference of the moving fluid modified by the transfer of momentum with the vortex field; it describes the evolution of a coherent vorticity structure. The vorticity structure would be conserved if $\frac{\partial\omega^i}{\partial t} + \mathcal{L}_{\lambda c_m u}\omega = 0$. Eq. (8) is similar to the NST expression obtained from Eq. (7) by setting $\lambda c_m = 1$ and by operating on both sides with the curl operator $\nabla\times$. The NST predicts only that the vorticity diffuses. In contrast, the present formulation shows that the vorticity and the vortex field are convected as well as diffused. This is one reason for the persistence of the Dean vortex emitted from a helical pipe into a straight section [7].

Finally, a detailed analysis of the interaction of the vortex field at intermediate speeds leads to a new dissipation mechanism that takes the form

$$\zeta \equiv \sigma^{-1} j = \frac{\sigma^{-1}\bar{\eta}}{4\pi}\kappa\nabla\times\omega, \tag{9}$$

where the "resistance" is given by $\sigma^{-1} = \frac{4\pi\eta}{\kappa\rho\bar{\eta}}$. The physical consequence of the resistance is that energy dissipation in the vortex field can be slowed by high resistance. This limits the transfer of inertial energy-momentum to/from the vortex field in this intermediate speed range. This is a vortex field lifetime effect, different from an energy dissipation. For the low speed limit, we find no such rate limiting. Consequently, after a vortex field is built-up, on moving down stream, it decays at a diminished rate. This allows a vortex field, built-up in one part of the flow, to be convected to other parts of the flow. Such a mechanism provides the final piece of the story for the long lived vortex field downstream of the helical pipe outlet that persists in the straight pipe for more than a thousand diameters [7]. The energy dissipation results involve integrals over the vortex field. The effects of the vortex field can also be measured in terms of the velocity field and the lifetimes of transverse wave excitations and compared to GFD predictions. These would quantitatively differ from those of NST.

In summary, the Letter presents a classical acoustic spacetime field theory of a Newtonian fluid, self-excited by a fluid vortex field. Mathematically, in SASTs there *must* exist a vortex field for time varying velocity fields. The wave structure and energy dissipation found in experiments is consistent with the excitation of transverse vorticity (TV) and transverse swirl (TS) waves due to the

vortex field. The experimental results for energy dissipation were also in agreement with the theory.

References

[1] W. G Unruh, Phys. Rev. Lett. 46 (1981) 1351.
[2] W.G. Unruh, Phys. Rev. D 51 (1995) 2827.
[3] C. Barcelo, Living Rev. Rel. 8 (2005) 12.
[4] D.F. Scofield, P. Huq, Phys. Lett. A 372 (2008) 4474.
[5] C.M. White, Proc. R. Soc. A 123 (1929) 645.
[6] G.I. Taylor, Proc. R. Soc. A 124 (1929) 243.
[7] K.R. Sreenivasan, P.S. Strykowski, Exp. Fluids 1 (1983) 31.
[8] R. Narasimha, K.R. Sreenivasan, Adv. Appl. Mech. 19 (1979) 221.
[9] M. Anwer, R.M.C. So, Y.G. Lai, Phys. Fluids A 1 (1989) 1387.
[10] M. Kurokawa, K.C. Cheng, L. Shi, J. Visualization 1 (1998) 1.
[11] L.D. Landau, E.M. Lifschitz, Fluid Mechanics, transl. J.B. Sykes and W.H. Reid, Pergamon Press, London, 1959.
[12] N.H. Scott, Wave Motion 22 (1995) 335.
[13] J.A. Stratton, Electromagnetic Theory, McGraw–Hill, New York, 1941.
[14] H. Flanders, Differential Forms with Applications to the Physical Sciences, Dover, New York, 1989.
[15] C.W. Misner, K.S. Thorn, J.A. Wheeler, Gravitation, Freeman, San Francisco, CA, 1973.
[16] R.M. Kiehn, Non-Equilibrium Thermodynamics, vols. 1–5, Lulu Enterprises, Morrisville, NC, 2007.
[17] J.D. Jackson, Classical Electrodynamics, third ed., John Wiley & Sons, New York, 1998.
[18] S.A. Berger, L. Talbot, L.S. Yao, Annu. Rev. Fluid Mech. 15 (1983) 461.
[19] B. Hof, C.W.H. van Doorne, J. Westerweel, F.T.M. Nieuwstadt, H. Faisst, B. Eckhardt, H. Wedin, R.R. Kerswell, F. Waleffe, Science 305 (2004) 1594.
[20] B. Hof, T. Mullin, Phys. Rev. Lett. 91 (2003) 244502.
[21] H. Faisst, B. Eckhardt, Phys. Rev. Lett. 91 (2003) 224502.
[22] B. Eckhardt, Nonlinearity 21 (2008) T1.
[23] B. Eckhardt, T.M. Schneider, B. Hof, J. Westerweel, Annu. Rev. Fluid Mech. 39 (2007) 447.
[24] H. Wedin, R.R. Kerswell, J. Fluid Mech. 508 (2004) 333.
[25] R.R. Kerswell, Nonlinearity 18 (2005) R17.